THEORETICA CHIMICA ACTA

Theoret. Chim. Acta (Berl.) 61, 149–162 (1982)

Perturbative Solution of the RPA Equation. An Application to the Calculation of Rotational Strengths

Jean-Pierre Flament and Henri-Pierre Gervais

Groupe de Chimie Théorique, Laboratoire de Synthèse Organique, Ecole Polytechnique, F-91128 Palaiseau, France

The RPA equation is solved by perturbation in Møller–Plesset (MP) and Epstein–Nesbet (EN) partitions, which are first compared on a specific example. To still accelerate the faster one (EN), a third scheme is proposed, which involves preliminary diagonalization within a limited subset $\mathbb{S}$, followed by usual EN perturbation between $\mathbb{S}$ and the rest of the whole configuration space. Criteria for the choice of $\mathbb{S}$ are given.

Key words: Perturbation theory – RPA – Rotational strengths – Carbonyl chromophores – Norcamphor.

1. Introduction

For a satisfactory description of electronic spectra one needs to introduce electronic correlation, either via configuration interaction (CI) [6–9] for the separate calculations of the states concerned, or via the more direct procedure using Equations-of-Motion (EOM) [15, 30] (Random Phase Approximation, (RPA) [10–12] or in more sophisticated approximations [30b, c]). Even for small molecules, of course, one is soon faced with problems related to the size of the basis set: restriction of the CI or RPA to a limited number of low-lying configurations usually leads to reasonable transition energies, but this becomes a daring attempt when one has to calculate quantities like the rotational strength [R], [1–4], which are very sensitive to the quality of the wave functions; in this specific case, modification of the basis may lead to results differing both in sign and amplitude [8, 12]! Volosov and Zubkov [8] have discussed the influence of

Offprint requests and correspondence to J.-P. Flament.

0040-5744/82/0061/0149/$02.80

the CI size on the value of $[R]$ and given a recipe for semi-empirical calculations: they propose to deal with only half of the full basis (limited to energy-ordered monoexcitations) when $[R]$ oscillates as the size varies, and with a hundred of configurations in well-behaved cases.

In this paper, we investigate the behaviour of rotational strengths during CNDO/S – RPA or *ab initio* – RPA calculations and we show how the RPA eigenvalues can be determined perturbatively to deal with the whole basis set.

2. Method of Calculation

Diagonalization of the RPA matrix by the standard method [13–14] becomes a considerable task when the basis set increases. Moreover, spectroscopists are generally interested only in the few lowest transitions, without need of all the eigenvalues. Although some existing procedures are appropriate for this case [25], one can also tentatively turn to the perturbation scheme, to which the problem may be reduced in most cases for ground state calculations; unfortunately it soon appears that, in RPA, numerators and denominators involved in the perturbation formulas may be of the same order of magnitude, so that the underlying assumptions of perturbation theory no longer apply. We shall see, however, that reorganization of the basis set and convenient choice of the zero-order superoperator hamiltonian are able to accelerate the convergence of the perturbation series.

2.1. Perturbation Theory for RPA

2.1.1. General equations

Simons and Jørgensen [15] have shown that:
(a) analysis of the EOM within the framework of perturbation theory leads to the same formal relations as the usual Rayleigh–Schrödinger scheme;
(b) completeness of the basis set requires inclusion of both the excitation operators $|O_j^+)$ and the associated deexcitation operators $|O_j)$, with the closure relation:

$$1 = \sum_j (|O_j^+)(O_j^+| - |O_j)(O_j|). \tag{1}$$

Assuming that the eigenoperators $|O_i^+)$ (eigenvalue ω_i) of the superoperator hamiltonian:

$$\mathscr{H} = \mathscr{H}_0 + \mathscr{R} \tag{2}$$

$$\mathscr{H}|O_i^+) = \omega_i |O_i^+) \tag{3}$$

can be developed as sums of terms of order 0 (corresponding to $\mathscr{H}_0$), 1, 2, . . . :

$$|O_i^+) = |O_i^+)_0 + \sum_{n \neq 0} |O_i^+)_n \tag{4a}$$

$$\omega_i = \omega_{i(0)} + \sum_{n\neq 0} \omega_{i(n)} \tag{4b}$$

one finds after collecting terms of the same order, as in the usual RSPT:

$$\mathcal{H}_0|O_i^+)_0 = \omega_{i(0)}|O_i^+)_0 \tag{5.0}$$

$$\mathcal{H}_0|O_i^+)_1 + \mathcal{R}|O_i^+)_0 = \omega_{i(0)}|O_i^+)_1 + \omega_{i(1)}|O_i^+)_0 \tag{5.1}$$

$$\vdots$$

$$\mathcal{H}_0|O_i^+)_n + \mathcal{R}|O_i^+)_{n-1} = \sum_{p=0}^{n} \omega_{i(p)}|O_i^+)_{n-p}. \tag{5.n}$$

Developing $|O_i^+)$ on the solutions of Eq. (5.0):

$$|O_i^+) = \sum_j ({}_0(O_j^+|O_i^+)|O_j^+)_0 - {}_0(O_j|O_i^+)|O_j)_0)$$

$$= \sum_j (Z_j|O_j^+)_0 - Y_j|O_j)_0). \tag{6}$$

Eqs. (5) give the corrections to $\omega_{i(0)}$ and $|O_i^+)_0$. As usual, the coefficient $Z_i = {}_0(O_i^+|O_i^+)$ is undetermined and we require the corrections $|O_i^+)_n$ to be orthogonal to $|O_i^+)_0$:

$${}_0(O_i^+|O_i^+) = 1$$

$${}_0(O_i^+|O_i^+)_n = 0 \quad \forall n \neq 0 \tag{7}$$

Bracketting[1] Eq. (5.n) with ${}_0(O_i^+|$ gives the n-order correction to $\omega_{i(0)}$ as function of the $(n-1)$-order correction to $|O_i^+)_0$:

$${}_0(O_i^+|\mathcal{R}|O_i^+)_{n-1} = \omega_{i(n)}. \tag{8}$$

Bracketting Eq. (5.n) with $(A| = {}_0(O_j^+|(j \neq i)$ or $(A| = {}_0(O_j|$, $\forall j$, gives the n-order correction to $|O_i^+)_0$ as function of lower order ones:

$$[\omega_{i(0)} - \omega_A(A|A)](A|O_i^+)_n = (A|\mathcal{R}|O_i^+)_{n-1} - \sum_{p=1}^{n-1} \omega_{i(p)}(A|O_i^+)_{n-p}. \tag{9}$$

Explicit expressions up to order 3 are given in the Appendix.

2.1.2. Choice of $\mathcal{H}_0$: MP and EN schemes

The operators $Q_\mu^+ = q_{m\alpha}^+ = a_m^+ a_\alpha$ (m = particle, α = hole) or their spin-adapted equivalents ${}^S_M Q_\mu^+$, which form the basis set in the RPA scheme, are usually obtained through an SCF calculation.

A natural choice for $\mathcal{H}_0$ is then $\mathcal{F}$, superoperator associated with the Hartree–Fock hamiltonian F:

$$F = \sum_i \varepsilon_i a_i^+ a_i. \tag{10}$$

[1] in RPA the bracket is defined by $(A|\mathcal{H}|B) = \langle \mathrm{HF}|[A^+, [H, B]]|\mathrm{HF}\rangle$ and A and B are $1p$–$1h$ operators.

This corresponds exactly, in the operator space, to the so-called Møller–Plesset (MP) partition [16, 17] in the ordinary ket-space. The above $q^+_{m\alpha}$ (or ${}^{S}_{M}Q^+_{m\alpha}$) are just the eigenoperators of $\mathscr{H}_0 = \mathscr{F}$:

$$\mathscr{H}_0|q^+_{m\alpha}) = \omega_{m\alpha}|q^+_{m\alpha}) = (\varepsilon_m - \varepsilon_\alpha)|q^+_{m\alpha}) \tag{11}$$

or (see Eqs (8) and (9) for $n = 0$):

$$(Q^+_\mu|\mathscr{F}|Q^+_\nu) = \delta_{\mu\nu}\omega_\mu \qquad (\omega_\mu > 0). \tag{12}$$

But $\mathscr{F}$ is not the only superoperator having these Q^+_μ as eigenoperators. We can as well use a superoperator $\mathscr{H}'_0$ possessing eigenvalues $A_{\mu\mu}$ equal to the diagonal elements of the exact one $\mathscr{H}$, in the $\{A_\mu\}$ (A_μ is a general notation for Q^+_μ and Q_μ) basis:

$$\begin{aligned} A_{\mu\mu} &= (Q^+_\mu|\mathscr{H}|Q^+_\mu) \\ &= (A_\mu|\mathscr{H}|A_\mu). \end{aligned}$$

In this second scheme, called Epstein–Nesbet (EN) partition [17, 18], the diagonal elements of the perturbation superoperator $\mathscr{R}'$ reduce to zero.

We can define the superoperators involved in both partitions, by their matrix elements in the $\{A_\mu\} = \{Q^+_\mu, Q_\mu\}$ basis, and schematize the whole as in Figs. 1 and 2:

(a) $\mathscr{H} = \mathscr{F} + \mathscr{R}$ (Møller–Plesset)

$$\begin{aligned} &(A_\mu|\mathscr{F}|A_\nu) = \delta_{\mu\nu}\omega_\mu = \delta_{\mu\nu}(\varepsilon_m - \varepsilon_\alpha) \qquad (\mu = [m\alpha]) \\ &(A_\mu|\mathscr{R}|A_\mu) = (A_\mu|\mathscr{H}|A_\mu) - (A_\mu|\mathscr{F}|A_\mu) \end{aligned} \tag{13}$$

(b) $\mathscr{H} = \mathscr{H}'_0 + \mathscr{R}'$ (Epstein–Nesbet)

$$\begin{aligned} &(A_\mu|\mathscr{H}_0|A_\mu) = (A_\mu|\mathscr{H}|A_\mu) \\ &(A_\mu|\mathscr{H}_0|A_\nu) = 0 \\ &(A_\mu|\mathscr{R}'|A_\mu) = 0 \\ &(A_\mu|\mathscr{R}'|A_\nu) = (A_\mu|\mathscr{H}|A_\nu) = (A_\mu|\mathscr{R}|A_\nu). \end{aligned} \tag{14}$$

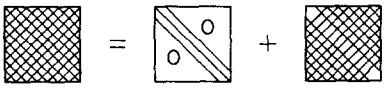

Fig. 1. Møller–Plesset (MP) partition

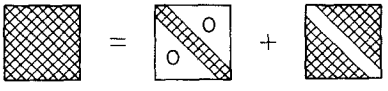

Fig. 2. Epstein–Nesbet (EN) partition

2.1.3. Comparison of convergences

(a) Comparison at second order. Suppose we are interested in some particular transition, associated with operator $|O_i^+)_0$ (eigenvalue $\omega_{i(0)} = \omega_0$) in the initial Hartree–Fock result. From the definitions of $\mathscr{H}_0$ and $\mathscr{H}'_0$, we first notice that the zero-order Epstein–Nesbet energy (ω'_0) already contains the first-order correction to the Møller–Plesset energy:

$$\omega'_0 = \omega_0 + \omega_1.$$

The first-order EN correction is zero (see Fig. 2), so that both partitions are equivalent, for *energy*, to first-order.

The EN correction to energy starts at second order, with[2]:

$$\omega'_{i(2)} = \sum_{\mu \neq i} \frac{|{}_0(Q_\mu^+|\mathscr{R}|O_i^+)_0|^2}{\omega'_{i(0)} - \omega'_{\mu(0)}} - \sum_{\mu} \frac{|{}_0(Q_\mu|\mathscr{R}|O_i^+)_0|^2}{\omega'_{i(0)} + \omega'_{\mu(0)}}$$
$$= \omega'_{i(2)}(Q^+) + \omega'_{i(2)}(Q) \tag{15}$$

and we have, from Eq. (14):

$$\omega'_{i(0)} - \omega'_{\mu(0)} = \omega_{i(0)} - \omega_{\mu(0)} + {}_0(O_i^+|\mathscr{R}|O_i^+)_0 - {}_0(Q_\mu^+|\mathscr{R}|Q_\mu^+)_0$$

$$\frac{1}{\omega'_{i(0)} - \omega'_{\mu(0)}} = \frac{1}{\omega_{i(0)} - \omega_{\mu(0)}} \left[1 + \frac{{}_0(Q_\mu^+|\mathscr{R}|Q_\mu^+)_0}{\omega_{i(0)} - \omega_{\mu(0)}} - \frac{{}_0(O_i^+|\mathscr{R}|O_i^+)_0}{\omega_{i(0)} - \omega_{\mu(0)}} + \cdots\right]$$

so that:

$$\omega'_{i(2)}(Q^+) = \sum_{\mu \neq i} \frac{|{}_0(Q_\mu^+|\mathscr{R}|O_i^+)_0|^2}{\omega_{i(0)} - \omega_{\mu(0)}} \left[1 + \frac{{}_0(Q_\mu^+|\mathscr{R}|Q_\mu^+)_0}{\omega_{i(0)} - \omega_{\mu(0)}} - \frac{{}_0(O_i^+|\mathscr{R}|O_i^+)_0}{\omega_{i(0)} - \omega_{\mu(0)}} + \cdots\right] \tag{16}$$

$$\omega'_{i(2)}(Q) = -\sum_{\mu} \frac{|{}_0(Q_\mu^+|\mathscr{R}|O_i^+)_0|^2}{\omega_{i(0)} - \omega_{\mu(0)}} \left[1 - \frac{{}_0(Q_\mu|\mathscr{R}|Q_\mu)_0}{\omega_{i(0)} + \omega_{\mu(0)}} - \frac{{}_0(O_i^+|\mathscr{R}|O_i^+)_0}{\omega_{i(0)} + \omega_{\mu(0)}} + \cdots\right]. \tag{17}$$

Clearly, the first terms in Eqs. (16) and (17) are the MP ω_2, and the next two ones are a part of ω_3. It is thus hoped that the EN partition will give faster convergence to the perturbation series.

(b) *Numerical illustration.* To test this assertion, we have performed a model calculation on a part of the RPA matrix relative to [2, 2, 1]bicycloheptan-2-one (norcamphor), built up from a CNDO/S [19] calculation of the ground state. The absolute molecular configuration is (1R, 4S) (Fig. 3); the geometry is given by X-ray diffraction [20] and we have optimized the position of hydrogens through a Westheimer-type procedure [21].

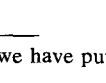

Fig. 3.

[2] Here we have put $|Q_\mu^+)_0$ ($\mu \neq i$) and $|Q_\mu)_0$ to distinguish $|O_i^+)_0$ from the other basis operators.

Table 1. Møller–Plesset partition

Perturbation order	Corrected energy	% error	Overlap	Exact energy (diagonalization)
0	0.455318	230	0.993720	0.137737 u.a.
1	0.141064	2.5	0.994323	
2	0.134864	2.08	0.993964	
3	0.140514	2.01	0.994125	
4	0.135223	1.82	0.993609	
5	0.140033	1.66	0.993106	

Table 2. Epstein–Nesbet partition

Perturbation order	Corrected energy	% error	Overlap
0	0.141064	2.5	0.99372
1	0.141064	2.5	0.999977
2	0.137749	$8.7 \cdot 10^{-3}$	0.999998
3	0.137734	$2.2 \cdot 10^{-3}$	0.999998
4	0.137736	$7 \cdot 10^{-4}$	0.999998
5	0.137737	0	0.999998

The truncated basis we used contains the 60 Q_μ^+ and 60 Q_μ obtained when exciting an electron from one of the three highest occupied MO's to one of the twenty virtual orbitals.

Tables 1 (MP partition) and 2 (EN partition) collect results relative to the transition energy, for the lowest ($n \to \pi^*$) transition; the last column gives the overlap between the excitation operator obtained in this case by perturbation and the "exact" one, given by direct diagonalization.

Clearly, the EN partition leads to faster convergence than the MP one (which gives rise to oscillations). But the exact value is reached only at fifth order, for a transition which is well isolated from the others. The aim of the method being to limit calculation to the first order (or at least to a low order), it is thus necessary to modify the basis set.

2.2. A Third Scheme

It involves a preliminary reorganization of the operator basis, in a spirit similar to that of the CIPSI method [22]. For the transition associated with operator $|Q_i^+)$ in the initial Hartree–Fock result, we no more restrict the zero-order operator to $|Q_i^+)_0 = |Q_i^+)$, as above: we first diagonalize the exact superoperator $\mathscr{H}$ within a limited basis $\mathbb{S}$, formed by operators *which interact strongly* (according to some criterion) with $|Q_i^+)$. This leads to a new partition in the EN scheme:

(1) in subspace $\mathbb{S}$ (dimension d), where diagonalization has been effected, the new basis operators are the eigenoperators of $\mathscr{H}$:

$$\mathscr{H}|O_i^+)_0 = \omega_{i_0}|O_i^+)_0 \tag{18a}$$

with

$$|O_i^+)_0 = \sum_{\mu=1}^{d} (Z_{\mu i}|Q_\mu^+) - Y_{\mu i}|Q_\mu)) \tag{18b}$$

the zero-order superoperator $\mathscr{H}_0''$ is defined by the new eigenvalues $\omega_{i(0)} = \omega_{i0}$; the new perturbation $\mathscr{R}''$ has zero matrix elements.

(2) in the complementary subspace $\mathbb{T}$, the basis is $\{Q_\mu^+, Q_\mu/Q_\mu^+,\ Q_\mu \notin \mathbb{S}\}$; $\mathscr{H}_0''$ and $\mathscr{R}''$ are defined as in 2.1.2 by:

$$(A_\mu|\mathscr{H}_0''|A_\mu) = (A_\mu|\mathscr{H}|A_\mu) \tag{19a}$$

$$(A_\mu|\mathscr{R}''|A_\nu) = (A_\mu|\mathscr{H}|A_\nu). \tag{19b}$$

(3) in the $\mathbb{S}$–$\mathbb{T}$ blocks, $\mathscr{H}_0''$ has zero elements while $\mathscr{R}''$ is given by:

$$(A_\mu|\mathscr{R}''|O_i^+)_0 = (A_\mu|\mathscr{H}|O_i^+)_0. \tag{20}$$

Account has thus been taken of the preliminary diagonalization in $\mathbb{S}$. This new partition scheme is visualized in Fig. 4:

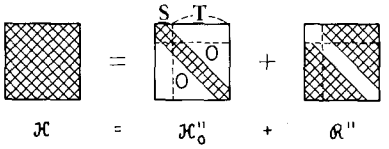

Fig. 4. Epstein–Nesbet perturbation after partial diagonalization

Remarks

(i) In the case of an MP partition, we would have for the $\mathbb{S}$ block of $\mathscr{H}$:

$$\omega_{i(0)} = \sum_{\mu=1}^{d} (Z_{\mu i}^2 + Y_{\mu i}^2)(\varepsilon_m - \varepsilon_\alpha) \qquad (\mu = [m\alpha]) \tag{21}$$

$$_0(O_i^+|\mathscr{R}|O_i^+)_0 = \omega_{i0} - \omega_{i(0)}$$

and expressions analogous to Eq. (13) or Eq. (20) for the $\mathbb{T}$ and $\mathbb{S}$–$\mathbb{T}$ blocks.

(ii) The schemes presented here dealt with the RPA in which the operator space is limited to $1p$–$1h$ operators, but we believe that it may be extended to include $2p$–$2h$ operators [15] in the same manner, or to problems which retain the RPA form.

3. Application of the Third Scheme to a Specific Example

We have tested the efficiency of the third scheme by computing the rotational strengths associated with the lowest transitions of bicyclo[2,2,1]heptan-2-one, a chiral ketone already presented in 2.1.3 (Fig. 3). As mentioned above, this is

a very good indicator for the quality of transition operators, because of the high sensitivity of $[R]$; this quantity is most conveniently computed in the dipole velocity form and expressed as the reduced rotational strength [23], so that we have for a transition $0 \rightarrow n$ starting from the fundamental electronic state:

$$[R_{on}] = 1.08 \cdot 10^{40} R_{CGS} = -\frac{254}{\omega_{0n}} \langle 0|\vec{\nabla}|n\rangle \cdot \langle n|\vec{r} \wedge \vec{\nabla}|0\rangle \tag{22}$$

where the energy and moments are given in atomic units. In Eq. (22), transition moments can be derived from those associated with the various configurations by using an expression similar to Eq. (6) for the transition operator $|O_i^+\rangle$:

$$\langle i|\nabla|O\rangle = \sqrt{2} \sum_{m\alpha} (Z_{m\alpha,i} - Y_{m\alpha,i}) \langle m|\nabla|\alpha\rangle \tag{23a}$$

$$\langle i|\boldsymbol{r} \wedge \nabla|O\rangle = \sqrt{2} \sum_{m\alpha} (Z_{m\alpha,i} - Y_{m\alpha,i}) \langle m|\boldsymbol{r} \wedge \nabla|\alpha\rangle. \tag{23b}$$

The necessary fermion operators were computed using both a CNDO/S or an *ab initio* STO-3G minimal basis calculation; in the CNDO/S case, the atomic integrals appearing in the development of (23a–b) were evaluated using Slater type orbitals approximated by STO-4G combinations [24] (use of STO-6G functions left the results essentially unchanged).

3.1. CNDO/S *Results for the Lowest Transition* $(n \rightarrow \pi^*)$

We first examine the behavior of $[R]$ with the size of the basis set, and the influence of the choice of $\mathbb{S}$ on the quality of the perturbation results, for the lowest $(n \rightarrow \pi^*)$ transition, which is well separated from the others. As already mentioned, the CNDO/S ground state of bicyclo[2,2,1]heptan-2-one contains 22 occupied MO'S (three of which were used in the numerical illustration of 2.1.3) and 20 virtual orbitals. We thus have done two types of calculations:

(1) a series of diagonalizations of the matrices obtained by successive enlargements of the configuration basis. The corresponding monoexcitations are generated automatically as follows:

First take all excitations from the highest occupied MO to the 20 successive virtual levels, with increasing ε_i:

Then create all excitations of similar nature, starting from the next highest occupied MO, etc... (final number of interacting configurations: NCI = 440).

Each time twenty new excitations have been generated, a diagonalization is performed by the method recently proposed [25], using the result of the previous diagonalization as initial operator.

(2) a series of perturbation calculations (*restricted to order* 1 *in the transition operator*, 2 in the transition energy), for various choices of the subspace $\mathbb{S}$. In this series, one fixes the excitations appearing in $\mathbb{S}$, while those forming $\mathbb{T}$ are generated in the same way as in case 1) (but by-passing the members of $\mathbb{S}$, of course). Four subspaces have been selected:

dimension 24
$\mathbb{S}_{24}$ is formed by the excitations which, in a previous calculation using a small-dimension $\mathbb{S}$, appeared with a coefficient Z greater than 10^{-2}.

dimension 29
$\mathbb{S}_{29}$ obeys the same criterion as $\mathbb{S}_{24}$, but with a test value of $7 \cdot 10^{-3}$.

dimension 40
$\mathbb{S}_{40}$ is formed in a similar way as $\mathbb{S}_{29}$, but strongly interacting excitations starting from the π orbital have been included.

dimension 41
Here $\mathbb{S}_{41}$ contains systematically all the mono-excitations associated with the HOMO and LUMO levels of the ground state, that is of types $n \rightarrow i^*$ (i^* any virtual orbital) and $j \rightarrow \pi^*$ (j any occupied MO). In this case, only two operators of $\mathbb{T}$ have Z superior to $5 \cdot 10^{-3}$.

Figure 5 shows the evolution of $[R]$ as function of the total number of monoexcitations (NCI) included in the calculation. From these diagrams, one can say that:

(a) the "diagonalization" line suffers considerable oscillations (the extremal values, not represented in fig. 5, are -23 and $+15$). The value -23 corresponds to the twenty excitations starting from the n orbital; the next twenty ones start from the π orbital, with a dramatic effect since it changes the sign of $[R]$.

(b) the "perturbation" lines show less pronounced oscillations, because some of the operators with a large Z are already included in $\mathbb{S}$. But examples 24 and

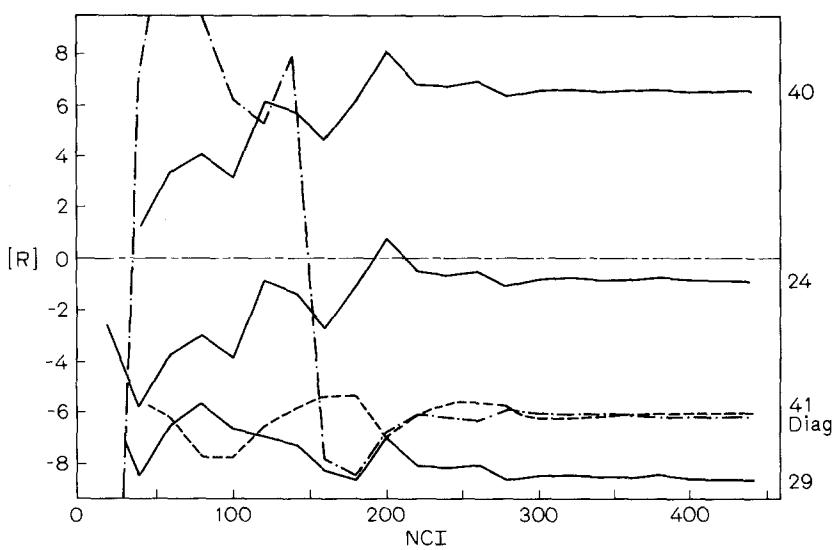

Fig. 5. Variation of $[R]$ with the number of configurations (NCI) (CNDO/S; transition $n \rightarrow \pi^*$). – · – · – by direct diagonalization; ——— by perturbation (order 1; dimensions 24, 29 and 40 for subspace $\mathbb{S}$); · · · · · · by perturbation (order 1; dimension 41 for $\mathbb{S}$). (The numbers on the right indicate the dimension of $\mathbb{S}$)

29 demonstrate clearly that the criterion relative to coefficient Z must be severe if one wants accurate values of $[R]$.

(c) curve 41 shows that this choice was good; the value of $[R]$ for the complete basis ($NCI = 440$; and remember that this is a perturbation *to order 1 only*, in the transition operator) is -5.967, which compares very favourably with the value of -6.252 obtained by diagonalization.

(d) comparing curves 40 and 41, it appears that the dimension of $\mathbb{S}$ is not a sufficient criterion to ensure a good value of $[R]$: some configurations (like the $\pi \rightarrow i^*$ ones) are finally unimportant as concerns coefficients Z and Y, but give rise to large values of $[R]$; in a small or unappropriate basis, they may have overestimated coefficients and then induce exaggerated effects which cannot be compensated (at order 1) by the remainder of the configuration set.

It is thus recommended to do this type of calculation step by step, enlarging subspace $\mathbb{S}$ by progressively decreasing the test on Z and Y; a final value of about $5 \cdot 10^{-3}$ is necessary to get fairly accurate results for $[R]$.

3.2. CNDO/S *and ab initio Results for the Four Lowest Transitions*

All the results in 3.1 concerned the lowest ($n \rightarrow \pi^*$) transition, which is well separated from the others. We now turn to the treatment of several transitions at a time; the corresponding calculations were done in the CNDO/S and *ab initio* minimal basis (STO/3G with standard exponents [24], on account of the size of the molecule).

At the beginning of this larger problem, the subspace $\mathbb{S}$ was so chosen as to contain the 25 (CNDO/S) or 20 (*ab initio*) first excitations (according to the ordering of diagonal elements); the test value β on the coefficients was then decreased in four steps, from 0.05 to a limit of 0.005 (the value β used at one iteration was that of the previous step, diminished by at least 0.016). Results obtained in each case after complete EN perturbation (at order *one* in the transition operators) are given in Fig. 6 (*ab initio*) and 7 (CNDO/S), where the numbers in abscissa indicate the dimension of $\mathbb{S}$ (d) and the value of β. The straight lines correspond to the values obtained by diagonalization, using the MOR method [25], and with simultaneous optimization of all the operators, as proposed by Raffenetti for CI [26] (the first three solutions of the CNDO problem were attained in respectively 12, 42 and 142 iterations by MOR [25], while Raffenetti's procedure gave the first four solutions in respectively 5, 9, 10 and 15 iterations).

As results from Figs. 6 and 7, convergence is observed for the four transitions at $\beta = 0.005$ in the *ab initio* computation, but difficult to obtain in the CNDO/S case for the two highest transitions, which need a quite large $\mathbb{S}$ because of the excessive number of configurations involved in their description (notice that the absolute values of $[R]$ observed in CNDO/S are rather poor, but the sign is correct). In the same way, the *ab initio* value for the ($n \rightarrow \pi^*$) lowest transition

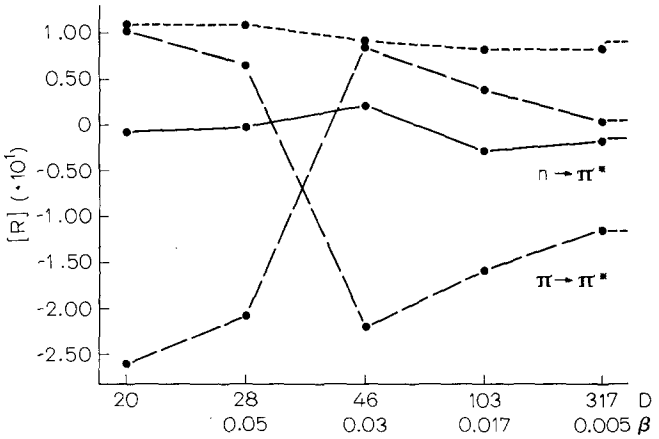

Fig. 6. Variation of $[R]$ with subspace $\mathbb{S}$ (dimension D; test value β): ab initio calculation

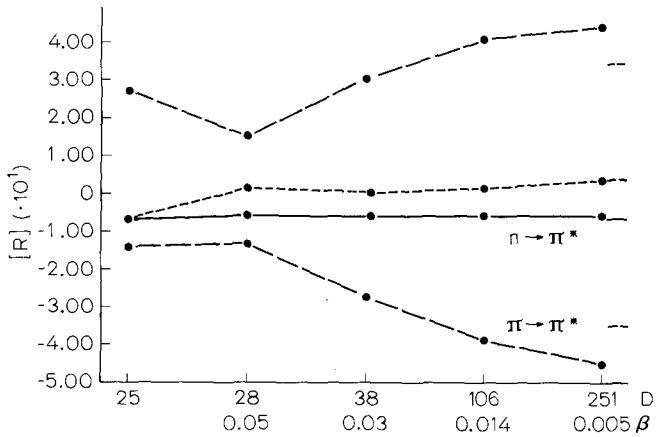

Fig. 7. Variation of $[R]$ with subspace $\mathbb{S}$ (dimension D; test value β): CNDO/S calculation

oscillates dramatically before the last iteration[3]: in fact this transition is better described than the others at step 0, and the first iterations artificially bring into $\mathbb{S}$ excitations that should mainly participate in the other transitions; only when β becomes small enough will all operators be finally treated upon the same footing.

All transition energies (not represented in Figures 6 and 7, but available upon request) were correct within 0.02 eV at step 2 ($\beta \approx 0.03$).

[3] When studying only this transition, a reasonable value of -1.89 is obtained in three iterations (NCI = 27, $\beta = 0.005$)

Remarks
(i) The MP partition gave poorer results; in particular, adopting a smaller value of 0.003 for the limit of β, we still got a wrong sign for the fourth transition in the ab initio case.
(ii) Both CNDO/S and *ab initio* calculations give the same sign for the final rotational strength of the lowest ($n \to \pi^*$) transition; this sign agrees with the Octant Rule's prevision [27], but not with the experimentally observed one at room temperature [28]. This is not surprising, because the experimental $[R]$ varies considerably with temperature, mainly due to vibronic effects [29] that may mask the exact equilibrium value. Results presented throughout this paper, and which are purely non-vibronic, support this point of view.

4. Conclusion

Calculations on bicyclo [2,2,1] heptan-2-one show that the rotational strength (a very sensitive observable taken as an indicator of the accuracy of transition operators) strongly depends on the size of the RPA basis. The problem can be dealt with by perturbation techniques, provided that the zero-order superhamiltonian has been properly chosen; but the Epstein–Nesbet partition gives better results than the Møller–Plesset one, which may lead to a wrong sign when the absolute value is small.

For a well-isolated transition, with a dominant configuration ($n \to \pi^*$ for instance), Volosov and Zubkov's prescription [8] (include all $n \to i^*$ and $j \to \pi^*$ in $\mathbb{S}$) gives accurate results.

When dealing with several states, or states without dominant configuration, good values are obtained by progressive enlargement of subspace $\mathbb{S}$, though a decrease in the test value β for the coefficients and provided that its ultimate limit is about $5 \cdot 10^{-3}$ (thus far from the value of 0.1 used by some authors [7]).

Appendix

1st Order

$$\omega_{i(1)} = {}_0(O_i^+|\mathcal{R}|O_i^+)_0$$

$${}_0(O_j^+|O_i^+)_1 = \frac{{}_0(O_j^+|\mathcal{R}|O_i^+)_0}{\omega_{i(0)} - \omega_{j(0)}}$$

$${}_0(O_j|O_i^+)_1 = \frac{{}_0(O_j|\mathcal{R}|O_i^+)_0}{\omega_{i(0)} + \omega_{j(0)}}.$$

2nd Order

$$\omega_{i(2)} = \sum_{j \neq i} \frac{|{}_0(O_j^+|\mathcal{R}|O_i^+)_0|^2}{\omega_{i(0)} - \omega_{j(0)}} - \sum_j \frac{|{}_0(O_j|\mathcal{R}|O_i^+)_0|^2}{\omega_{i(0)} + \omega_{j(0)}}$$

$$
{}_0(O_j^+|O_i^+)_2 = \sum_{k\neq i} \frac{{}_0(O_j^+|\mathscr{R}|O_k^+)_0\,{}_0(O_k^+|\mathscr{R}|O_i^+)_0}{(\omega_{i(0)}-\omega_{j(0)})(\omega_{i(0)}-\omega_{k(0)})} - \sum_k \frac{{}_0(O_j^+|\mathscr{R}|O_k)_0\,{}_0(O_k|\mathscr{R}|O_i^+)_0}{(\omega_{i(0)}-\omega_{j(0)})(\omega_{i(0)}+\omega_{k(0)})}
$$

$$
- {}_0(O_i^+|\mathscr{R}|O_i^+)_0 \frac{{}_0(O_j^+|\mathscr{R}|O_i^+)_0}{(\omega_{i(0)}-\omega_{j(0)})^2}
$$

$$
{}_0(O_j|O_i^+)_2 = \sum_{k\neq i} \frac{{}_0(O_j|\mathscr{R}|O_k^+)_0\,{}_0(O_k^+|\mathscr{R}|O_i^+)_0}{(\omega_{i(0)}+\omega_{j(0)})(\omega_{i(0)}-\omega_{k(0)})} - \sum_k \frac{{}_0(O_j|\mathscr{R}|O_k)_0\,{}_0(O_k|\mathscr{R}|O_i^+)_0}{(\omega_{i(0)}+\omega_{j(0)})(\omega_{i(0)}+\omega_{k(0)})}
$$

$$
- {}_0(O_i^+|\mathscr{R}|O_i^+)_0 \frac{{}_0(O_j|\mathscr{R}|O_i^+)_0}{(\omega_{i(0)}+\omega_{j(0)})^2}.
$$

3rd Order

$$
\omega_{i(3)} = \sum_{k\neq i}\sum_{l\neq i} \frac{{}_0(O_i^+|\mathscr{R}|O_k^+)_0\,{}_0(O_k^+|\mathscr{R}|O_l^+)_0\,{}_0(O_l^+|\mathscr{R}|O_i^+)_0}{(\omega_{i(0)}-\omega_{k(0)})(\omega_{i(0)}-\omega_{l(0)})}
$$

$$
-2\sum_{k\neq i}\sum_l \frac{{}_0(O_i^+|\mathscr{R}|O_k^+)_0\,{}_0(O_k^+|\mathscr{R}|O_l)_0\,{}_0(O_l|\mathscr{R}|O_i^+)_0}{(\omega_{i(0)}-\omega_{k(0)})(\omega_{i(0)}+\omega_{l(0)})}
$$

$$
+\sum_k\sum_l \frac{{}_0(O_i^+|\mathscr{R}|O_k)_0\,{}_0(O_k|\mathscr{R}|O_l)_0\,{}_0(O_l|\mathscr{R}|O_i^+)_0}{(\omega_{i(0)}+\omega_{k(0)})(\omega_{i(0)}+\omega_{l(0)})}
$$

$$
- {}_0(O_i^+|\mathscr{R}|O_i^+)_0 \left[\sum_{k\neq i} \frac{|{}_0(O_k^+|\mathscr{R}|O_i^+)_0|^2}{(\omega_{i(0)}-\omega_{k(0)})^2} - \sum_k \frac{|{}_0(O_k|\mathscr{R}|O_i^+)_0|^2}{(\omega_{i(0)}+\omega_{k(0)})^2}\right].
$$

References

1. Pao, Y. H., Santry, D. P.: J. Am. Chem. Soc. **88**, 4157 (1966)
2. Gould, R. R., Hoffmann, R.: J. Am. Chem. Soc. **92**, 1813 (1970)
3. Richardson, F. S., Shillady, D. D., Bloor, J. E.: J. Phys. Chem. **75**, 2466 (1971)
4. Imamura, A., Irano, T., Nagata, C., Tsuruta, T.: Bull. Chem. Soc. Japan **45**, 396 (1972)
5. Yaris, M., Moscowitz, A., Berry, R. S.: J. Chem. Phys. **49**, 3150 (1968)
6. Rauk, A., Jarvie, J. O., Ichimura, H. Barriel, J. M.: J. Am. Chem. Soc. **97**, 5656 (1975)
7. Rauk, A., Barriel, J. M.: Chem. Phys. **25**, 409 (1977)
8. Volosov, A. P., Zubkov, V. A.: Theoret. Chim. Acta (Berl) **44**, 375 (1977)
9. Bouman, T. D., Lightner, D. A.: J. Am. Chem. Soc. **98**, 3145 (1976)
10. Bouman, T. D., Hansen, Aa.: J. Chem. Phys. **66**, 3460 (1977)
11. Bouman, T. D., Hansen, Aa.: Chem. Phys. Lett. **53**, 160 (1978)
12. Bouman, T. D., Voigt, B., Hansen, Aa: J. Am. Chem. Soc. **101**, 550 (1979)
13. Ullah, N., Rowe, D. J.: Nucl. Phys. **A 163**, 257 (1971)
14. Jørgensen, P., Linderberg, J.: Int. J. Quant. Chem. **4**, 587 (1970)
15. Simons, J., Jørgensen, P.: J. Chem. Phys. **64**, 1413 (1976)
16. Møller, C., Plesset, M. S.: Phys. Rev. **146**, 618 (1934)
17. Claverie, P., Diner, S., Malrieu, J. P.: Int. J. Quant. Chem. **1**, 751 (1967)
18. Nesbet, R. K.: Proc. Roy. Soc. **A 230**, 312, 322 (1955)
19. Del Bene, J. Jaffé, H. H.: J. Chem. Phys. **48**, 1807, 4050 (1968)
20. Allen, F. H., Rogers, D.: J. Chem. Soc. 632 (1971)
21. Désalbres, X.: Thèse d'Etat, Paris (1978)
22. Huron, B., Malrieu, J. P., Rancurel, P.: J. Chem. Phys. **58**, 5745 (1973)
23. Moscowitz, A.: Adv. Chem. Phys. **4**, 96 (1962)
24. Hehre, W. J., Stewart, R. F., Pople, J. A.: J. Chem. Phys. **51**, 2657 (1969)
25. Flament, J. P., Gervais, H. P.: Int. J. Quant. Chem. **16**, 1347 (1979)

26. Raffenetti, R. C.: J. Comput. Phys. **32**, 403 (1979)
27. Moffitt, W., Woodward, R. B., Moscowitz, A., Klyne, W., Djerassi, C.: J. Am. Chem. Soc. **83**, 4013 (1961)
28. Coulombeau, C., Rassat, A.: Bull. Soc. Chim. France 516 (1971)
29. Désalbres, X., Gervais, H. P.: J. Chim. Phys. **77**, 513 (1980)
30. (a) Rowe, D. J.: Rev. Mod. Phys., **40**, 153 (1968) (b) Shibuya, T. I., McKoy, V.: Phys. Rev. **A 2**, 2208 (1970) (c) Oddershede, J., Adv. Quant. Chem. **11**, 275 (1978)

Received August 25/November 20, 1981